

Shearing Stress and Faulting in the Pachmarhi

Dr. N.L. Dongre



ABSTRACT-The distributions of intensity and orientation of maximum shearing stress in typical stress systems at Pachmarhi are plotted on stereographic projections, in order to show the three-dimensional relationships. Mathematical expressions of these relationships as well as graphical methods of evaluation are given. Relationships of shearing stress to orientation of fault planes and orientation of net slip of fault are described in reference of Pachmarhi. Methods of studying the relationships of faults and shearing stress are also described.



The solid geometry of shearing stress carries important implications pertaining to faulting and structural deformation, yet it has received only slight attention by geologists. Schmidt (1938), Sander (1940), Anderson (1948), and others have utilized the principle in interpretations. Schmidt's paper is an excellent treatment of the geometry of shearing stress and, has served as corroboration ii of part of the present Study. The problem of stress analysis in three dimensions has been a source of many discrepancies and incomplete understanding. The stereographic projection is used here in an attempt to illustrate the three-dimensional aspect of the problem related to the Pachmarhi.

Shearing-stress intensity

The total stress on any plane in a stress system can be broken into two components, one normal to the plane and, the other parallel to the plane. These components are known as "normal stress and shearing stress," respectively.

The intensity of maximum shearing stress to which any plane in a homogeneous elastic body under stress is subjected to, can be expressed by the formula



$$S^2 = n_1^2 \cos^2 a^2 + n_2^2 \cos^2 b^2 + n_3^2 \cos^2 c^2 - (n_1 \cos a^2 + n_2 \cos b^2 + n_3 \cos c^2)^2,$$

Where s = shearing stress; n_1, n_2 and n_3 are the three the three principal stresses always at right angles with +ve values representing compression and —values representing tension: and $a, b,$ and c are the angles from n_1, n_2 and n_3 axes, respectively, to the plane's normal. The derivation of this formula can be found in publications by Nadai (1931), Bucher (1921), and others. In order to picture the variation of intensity of shearing stress with various orientations of planes in a stress system, the stereographic projection has been employed.

(Wong, Teng-fong, Robina H.C. Wong, K.T. Chau, and C.A. Tang 2006), By this projection method, which represents a hemisphere plotted on a circle (Ford. 1932; Fisher, 1941; Bucher, 1944), the planes can be plotted as points in a circle; the points represent the intersection of the planes' normals with the hemisphere's surface or, stated other way, the points of tangency of the planes and sphere. In all the stereographic diagrams, the lower hemisphere of the unit sphere is pictured. The intensity of shearing stress on a particular plane is plotted at the point representing the plane. (Palchik, V. 2006), the variation intensities can then be contoured to show a complete diagram of the variation of shearing stress intensity (fig. I).

If the intensity on numerous places in a stress system is to be determined, the following graphic solution, using Mohr's stress plane is more rapid than solution by the formula. In figure 2, *a*, is shown a relationship, which has been recognized by Mohr and used as part of the demonstration of his theory of rupture. Briefly, the diagram expresses the fact that in a stress system, as normal stress varies, shearing stress also varies and that a graph showing the relationship of these two variables is always an arc of a circle. Thus, when shearing stress is plotted on the ordinate, normal stress on the abscissa, arcs of circles result (Nadai, 1931, pp43-44). The three principal stresses, n_1, n_2 and n_3 , are plotted on the abscissa, as they also represent normal stress for three planes at right angles to the three principal stresses and, furthermore, there would be no component of shearing stress on these three planes. As shown in figure 2, *a*, each of the principal stresses is joined to the other two by semicircles which represent the three 90° arcs between the principal stress axes. Thus the largest circle (dotted) represents the arc between n_1 and n_2 ; and shows that, as normal stress varies from the value of n_3 , to the value of n_3 ; shearing stress changes from zero to a maximum and back to zero. The variation of shearing and normal stress is similar on the other two arcs $n_1 - n_2$ and $n_2 - n_3$. It will be noted that in Mohr's stress plane, any circular arc equals twice the angle of the corresponding arc of the stress system. Co-ordinates may be constructed in Mohr's circle by drawing circles concentric to the two smaller ones. They correspond in position to the co-ordinates shown in the octant of the stress system (*Fig. a, b*) ; dotted, dashed, and solid arcs correspond in figure 2, *a*, and *b*. With Mohr's stress plane and circles constructed, values of normal and shearing stress can be read off the abscissa and ordinate axes for anti-plane in the stress system.

Several features of the resulting patterns formed by the contours of shearing stress intensity are worthy of special note. Diagrams in figure 1, *a-e*, show that, maximum shearing stress is always present on planes 45° from n_1 and n_3 . On Mohr's stress plane, this is represented by the highest point on the largest semicircle. In figure I, *a*, the intermediate stress n_2 equals the least stress n_3 , and thus all planes 45° from n_3 , are subjected to maximum shearing stress. All these planes might be thought of as being tangent to a cone around the n_1 axis. This cone can be called "a cone of maxima".

In similar manner (fig 1, *e*), when n_2 is equal to n_1 , all planes forming angles of 45° with n_3 are subjected to maximum shearing stress. All these planes would be tangent to a cone around n_3 .

Figure I, *b-d*, shows patterns for gradation between figure 1, *a* and *e*, and in each the positions of the 45° cones are marked by dashed lines. When n_2 differs from either n_1 or n_3 , only one plane is subject to maximum shearing stress, that at 45° from n_1 and n_3 . As n_2 varies away from n_1 in value of the intensity of shearing on the cone of maxima around n_1 decreases and the intensity on the cone of maxima around n_3 increases. It will be noted also that on the 90° arcs between n_1 and n_2 , n_2 and n_3 , and n_1 and n_3 the maximum shearing stress on each is at the 45° position.

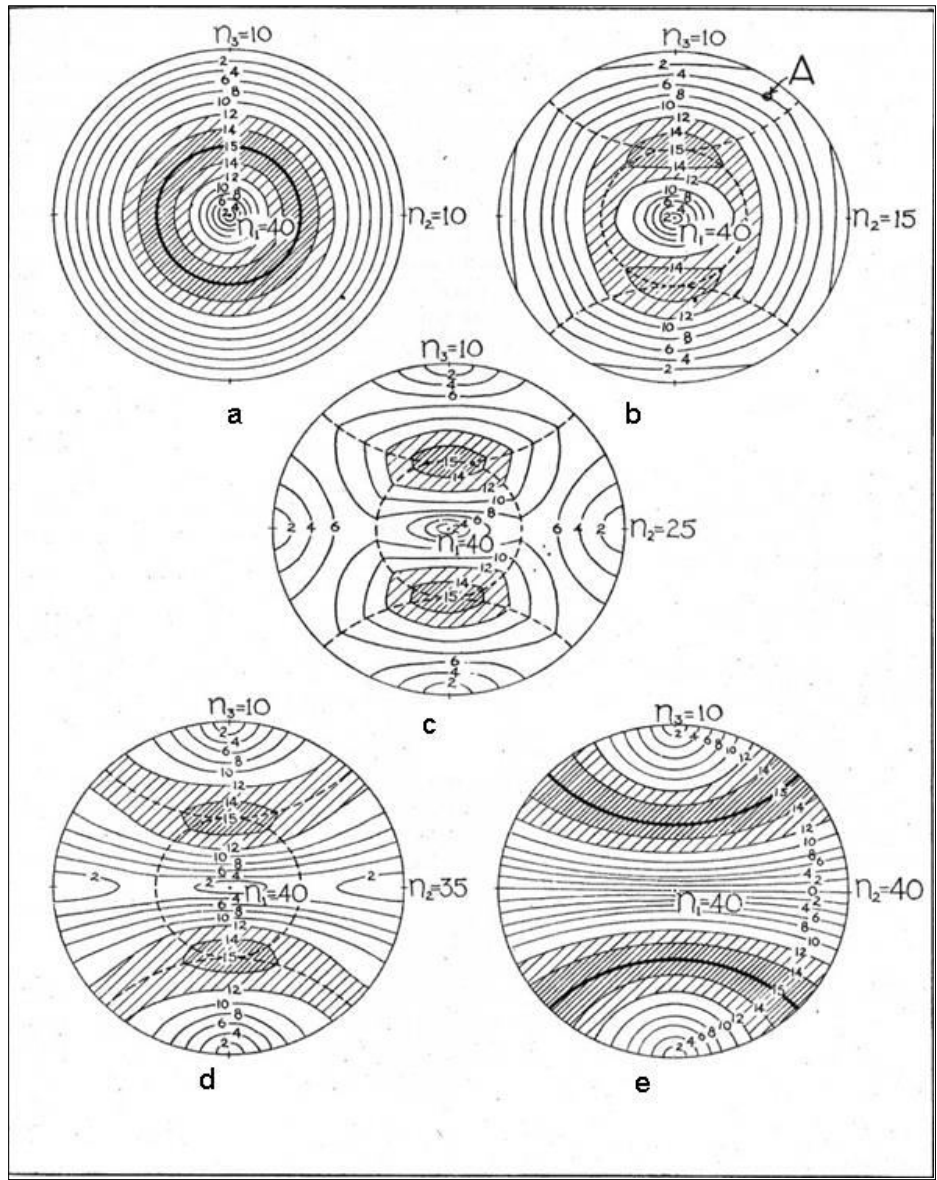


Figure.1-Intensities of shearing stress plotted on stereographic nets. N_1 , N_2 , and N_3 are principal axes. Intensity at any point represents shearing stress on a plane whose pole is that point (or a plane tangent to the sphere at that point). For example: Point A in figure b represents a plane striking N. 54° W. and dipping 84° SW., which is subjected to a shearing stress of 4 (lb/in², or whatever units are used) in this particular stress system. Dashed lines in a, b, c, and d represent, positions of cones around N_1 and N_3 . See text for explanation.

The situation in figure 1, a, might be called "uniaxia compression". There a force is applied in one principal axis and the confining forces on the other two are equal. In figure 1, e, the situation might be linked to uniaxial tension. The intensity and orientation of maximum shearing stress is governed only by the relative values of n_1 , n_2 and n_3 . Thus even if n_3 represents compression, if it is algebraically less than n_1 and n_2 the effect on shearing stress would be the same as if it were an axis of tension.

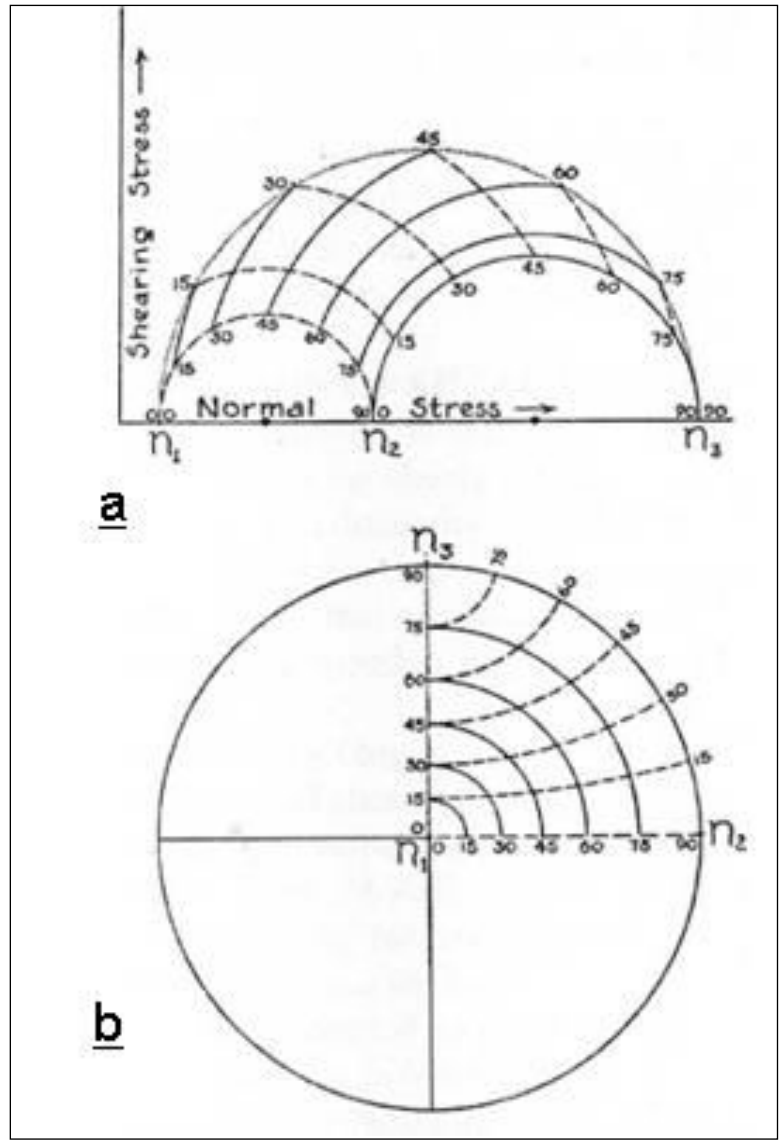


Figure.2- *a*, Mohr's stress plane, showing relation between shearing stress intensity and normal stress intensity in octant of a sphere, *b*, Octant of sphere plotted on stereographic net, showing relation of octant to Mohr's stress plane; dotted, dashed, and solid arcs correspond in *a* and *b*.

Orientation of maximum shearing stress

The variation of orientation of maximum shearing stress on different planes in different stress systems is shown in figure 3. In this figure it is perhaps easiest to picture any plane as tangent to the hemisphere, and the orientation of maximum shearing stress in the plane is represented by the arrow at that point. In the pattern in figure 3,a, where n_2 and n_3 , the orientation of maximum shearing stress on any plane can be thought of as parallel to the line of tangency between the plane and a cone around n_1 . Thus the arrows all point down, away from n_1 representing a "dip-slip" orientation on any plane. In figure 3, *e*, the orientation of maximum shearing stress on any plane is parallel to the line of tangency between the plane and a cone around n_3 . In the intermediate situations, figure 3, *b-d*, the orientation of maximum shearing stress varies between the two orientations indicated above. In figure 3, *b-d*, planes with very steep dips would have almost "strike-slip" orientation of maximum shearing stress, whereas as planes of low dip would have essentially "dip-slip" orientation. In figure 3, *b*, only the planes of steepest dip deviates greatly from "dip-slip" orientation of maximum shearing stress.

The orientation of maximum shearing stress on any plane in a given stress system may be expressed mathematically as follows:

$$\cos d = \frac{\cos s}{s} (n_1 - N),$$

$$\cos e = \frac{\cos s}{s} (n_2 - N),$$

$$\cos f = \frac{\cos s}{s} (n_3 - N),$$

Where, n_1, n_2 and n_3 are principal stresses; a, b and c are angles from the principal axes to the plane's normal; $d, e,$ and f are angles from the principal axes to the line of maximum shearing stress in the plane; S is the shearing-stress intensity; and N is the normal stress intensity.

The orientation of maximum Shearing stress may be determined graphically, as Shown in figure 4. In this diagram plotted the distribution of normal stress (values taken directly from Mohr's stress plane as illustrated in fig. 2). Shearing Stress as shown at sample points A and B is oriented at right angles to the contours of normal stress, or "down-gradient" of normal stress.

Relation of shear rupture

It is difficult to correlate conditions in the elastic state with conditions at and, after rupture, although it is the conditions in the elastic state that precede and lead to rupture. Any theory of rupture is confronted by this difficulty of correlation.

The present study of shearing stress is not a theory of rupture, for all that is concerned is a resolution of principal stresses into that component known as "shearing-stress". However a comparison of shearing stress and shearing rupture provides a useful basis for studying shearing rupture.

Experimental work described by Griggs (1936), Nadai (1931), and others has shown that the orientation of shearing rupture does not coincide with the planes of maximum shearing stress: rather, it develops on planes which form angles less than 45° with the axis of greatest compressive stress. Mohr's theory (Nadai 1931) includes both normal and shearing stress as governing factors to explain this variation of rupture planes from the 45° position of maximum shearing stress.

The following description is intended to point out that an angle of rupture less than 45° to the axis of maximum compression is quite expectable if shearing rupture is compared to friction problems, in which sliding or shearing depends both on the normal stress, tending to push the opposite parts together, and on the shearing stress, tending to slide the parts past one another.

Normal compressive stress on any plane in a stress system increases from zero to a maximum as the plane changes from an orientation, parallel to the axis of maximum compression to an orientation normal to that axis. (Riggs, Eric M. 2005), Thus less tangential stress (shearing stress) is required to cause shearing when the plane approaches an orientation parallel to the axis of greatest compressive stress. As normal stress varies from zero to a maximum, shearing stress changes from zero, reaches a maximum at 45° , and again becomes zero at 90° to the axis of greatest compression (see fig. 2), If normal stress were constant throughout the 90° arc, shearing rupture should develop at the orientation of maximum

shearing stress. The tendency is for the body to shear at an orientation representing a compromise between low normal stress and high shearing stress. This would always be at 45° or less with respect to the axis of maximum compression.

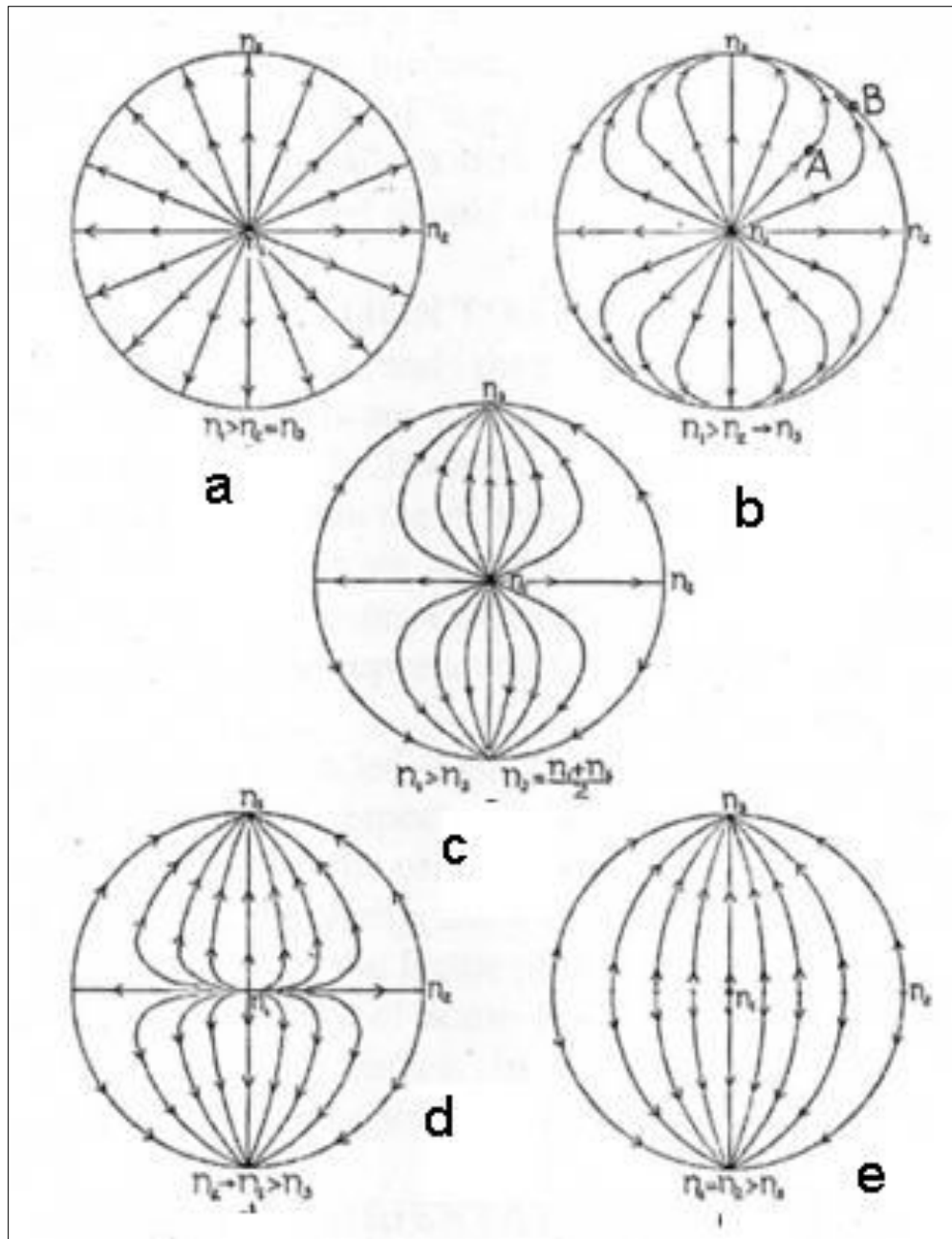


Figure.3- Orientation of maximum shearing stress plotted on stereographic nets. N_1 , N_2 and N_3 are principal stresses and correspond approximately to values in figure I. For example: Point A in figure b represents a plane striking N. 45° W. and dipping 65° SW. On this plane the orientation of maximum shearing stress is parallel to dip. Point B represents a vertical plane striking N. 45° W. On this plane the orientation of maximum shearing stress is parallel to strike

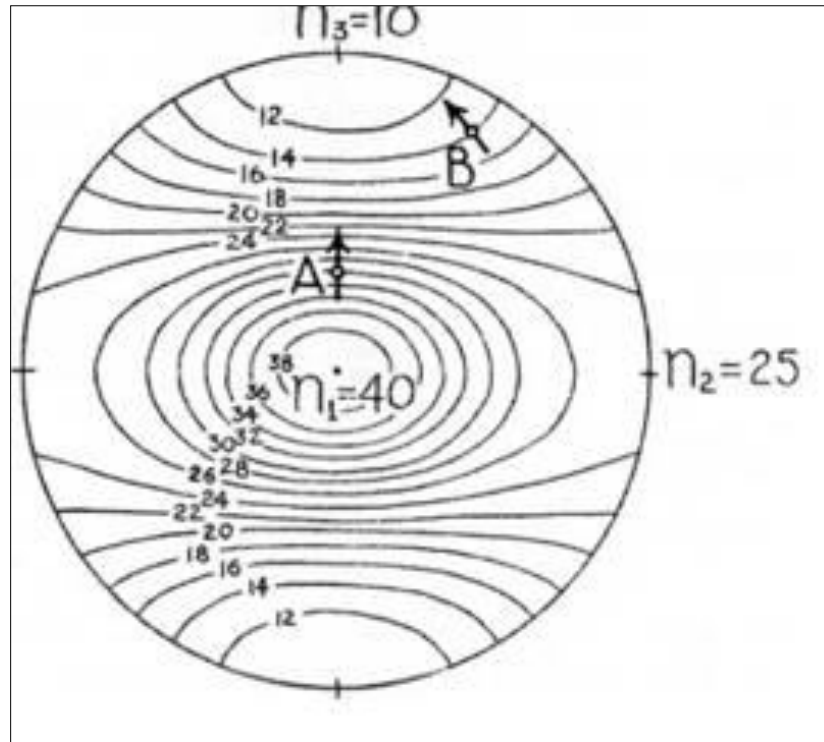


Figure . 4- Stereographic projection of normal stress, showing direction of maximum shearing stress to be "down gradient" of normal stress as at sample points A and B. Points N_1 , N_2 and N_3 are principal normal stresses.

Although shearing stress alone does not govern the angle of rupture, it is a basic consideration. The patterns shown in figure I represent only shearing stress intensities, but the patterns of "potential rupture" in a homogeneous body of infinite dimensions should be very similar, differing only by having the zones of maxima at angles slightly nearer n_1 . The variation would be dependent upon the material involved.

The correlation of orientation of maximum shearing stress with orientation of shearing motion in rupture is essentially a direct correlation. It should vary from perfect correlation at the instant of rupture and should diverge only as the elastic continuity of the material is destroyed.

Relation to faulting

Correlation of shearing stress and shearing rupture with faults in nature adds innumerable variables, which complicate the problem of analysis. Indeed, the variations possible are somewhat bewildering. Following are some major complicating factors. First, the shape of the tectonic blocks affects the distribution of shearing stress and orientation of rupture. Second, the strength anisotropism of rocks is of infinite variety. Third, the sequence of shifting orientations of stresses causing deformation is a factor very difficult to evaluate. Fourth, the distinction between shear rupture and tensional rupture in some cases is difficult to make.

In the present study, it is intended, first, to indicate the manner in which faults will follow preferred orientations with respect to the stresses and second, to indicate the relationship of net slip orientation to the orientation of the fault plane and the stress system. To do this with some degree of simplicity, three of the above-mentioned complicating variables are considered absent, and only the factor of strength anisotropism is retained. It would seem, upon considering the regularity of some fault systems, that this assumed degree of

simplicity is not too uncommon in nature. In the great majority of cases, a variety of complicating factors is present; but, to understand such complex situations, it is necessary first to understand the simpler cases.

Preferred orientations of faults

Faults will essentially follow a pattern of distribution similar to that of "rupture-potential" maxima discussed in the preceding section. In homogeneous rocks, faults will tend to concentrate at orientations tangent to a cone, with apex angle less than 90° (45° radius), which has the axis of greatest compressive stress as its axis; or tangent to a cone, with apex angle greater than 90° (45° radius), which has the axis of least compressive stress as its axis. (Wachter, L.M., C.E. Renshaw, and E.M. Schulson 2009),

Strength anisotropism of the rock can outweigh in effect the distribution of rupture potential in homogeneous rocks described above, and the resulting pattern of rupture can be drastically altered. An orientation of great weakness in the rock may well become a fault plane, although that particular orientation is subjected to far less shearing stress than any other orientations in the rock. In effect, a plane of almost any orientation may become a fault in non-homogeneous rocks, but the over-all grouping of orientations will tend to follow the two cone-like patterns described above.

An example follows to show how faults, apparently belonging to one stress system, may be correlated on the basis of orientation. Figure 5 shows by stereographic diagram how a group of faults in the Pachmarhi, fall roughly tangent to a cone with an apex angle slightly greater than 90° (or radius of 45°). N_3 is located by trial of various circles to find one which is most nearly tangent to all the faults. The angular center of this circle is then interpreted as being a principal stress axis-in this case the axis of least compressive stress because of the reverse nature of all faults.

The faults used in the example were observed in a mine tunnel where exposures were excellent and orientations of fault planes and relative displacements could be determined with a good degree of accuracy. Displacements on the faults range between 6 inches and 2 feet, and all are within a single large tectonic block measuring thousands of feet on a side. The rocks are massive, banded, limy argillites, which seem to have behaved as relatively homogeneous material. Bedding planes have not acted as planes of weakness but were very useful in determining the relative offset on the faults.

Orientation of net slip

Orientation of net slip on faults can be correlated almost directly with orientation of maximum shearing stress (fig. 3) as long as any continuity is maintained to the stress system after first rupture. The solid geometry of this relationship introduces complexities which are suggested by the following examples. Methods for dealing with certain aspects of the geometry are suggested.

Figure 6 shows by stereographic representation and map representation, how on three hypothetical faults, all striking the same way but of different dips, the net-slip orientation (heavy arrows) varies in three simple stress systems. This interpretation is taken directly from the patterns of orientation of maximum shearing stress shown in figure 3 and represents a direct correlation of net slip with maximum shearing stress for the purpose of illustration. In figure 7, a strike-slip fault, a reverse fault, and a normal fault result in a single uniaxial stress system, illustrating the complexity of net-slip orientations that can be produced in simple uniaxial stress systems,

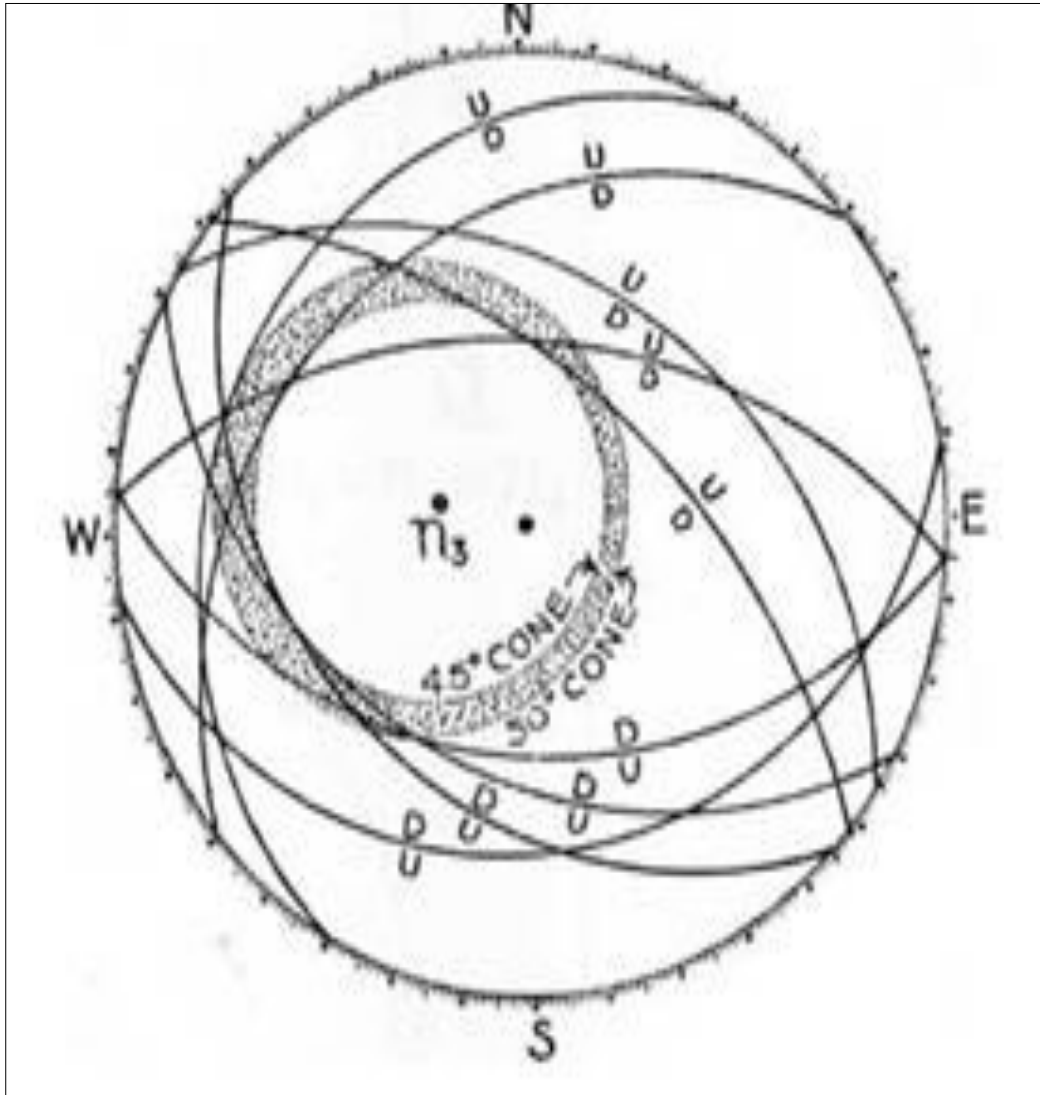


Figure. 5- Stereographic projection of faults (plotted as great circles) in Pachmarhi, showing possible relation to cones around axis of least compressive stress.

where orientation of the stress system is as shown in figure 3. The orientation of net slip on any plane can be readily determined from the diagrams. Where the stress system is tilted, this correlation is in some cases difficult to see without first rotating all planes and points into the orientation diagramed. It is in some cases useful to construct the resolved shearing-stress orientations for uniaxial tension and uniaxial compression. This provides two limits between which fall the orientations of maximum shearing stress for all cases where the values of the three principal stresses are different. As indicated previously, the orientations of maximum shearing stress in uniaxial tension and uniaxial compression parallel the line of tangency of the fault plane and a cone around either the axis of least or the axis of greatest compression. Thus, by constructing a circle (representing a cone) around the axis considered (see fig. 8), so that the circle is tangent to the fault plane (represented by the arc of a great circle), a line from the point of tangency to the sphere center represents the orientation of trend and plunge of maximum shearing stress. With the two limits determined, an approximation of the net-slip orientation can be made.

If a complete picture of fault-plane orientations and net-slip orientations on several faults is available, it should be possible to determine with some degree of certainty the

orientation and nature of the stress system producing the faults. If partial data are available, it may be possible to use this information in a limited prediction of the unknown factors. For example, if the orientations of several fault planes are known and it is believed that they are related to the same stress system, the orientations and relative movement of net slip on the various faults should have a definite relationship to one another and to the vault planes

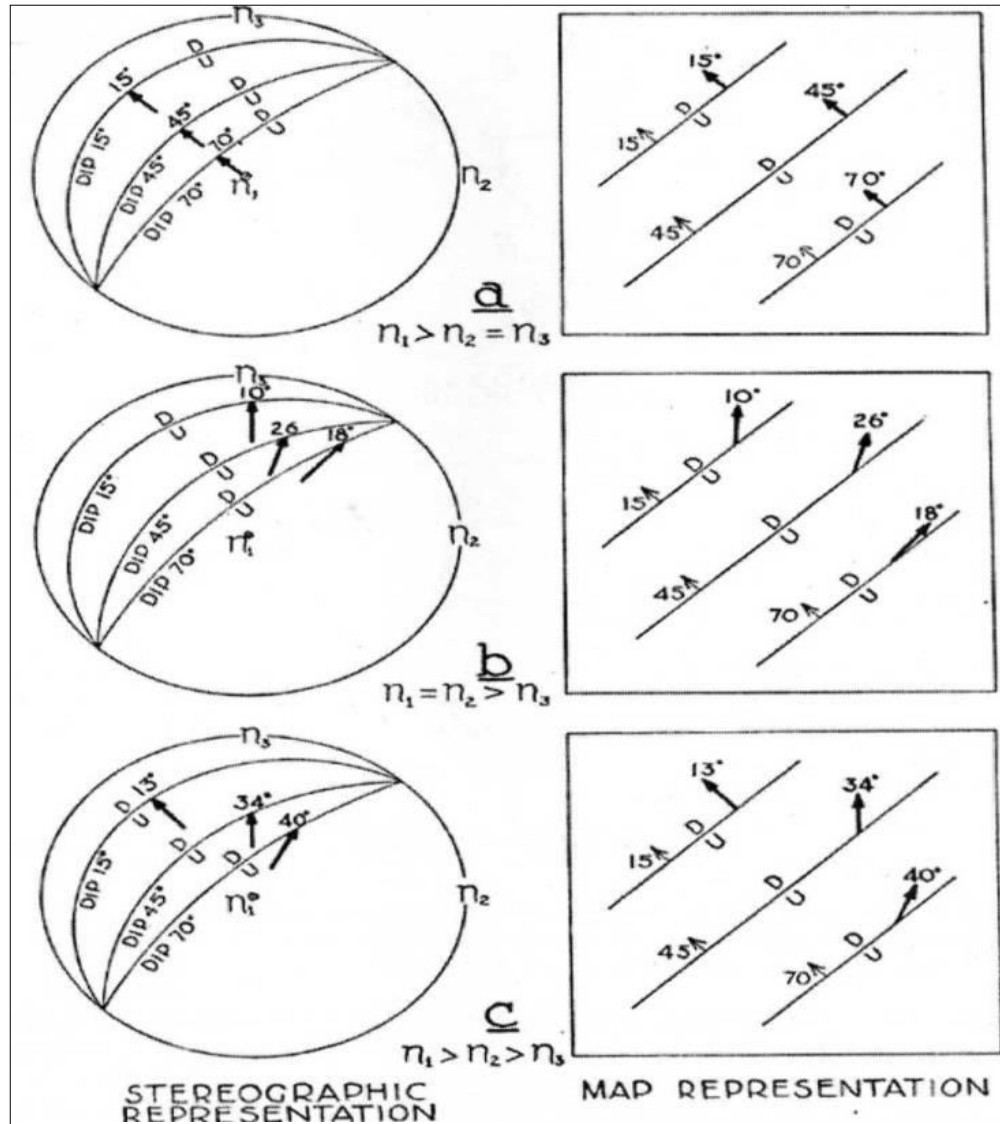


Figure. 6- Orientation of maximum shearing stress (heavy arrows) on three sample planes, in three stress systems shown in stereographic representation (left) and expressed as orientation of net slip on faults (right). N1 = axis of greatest compressive stress, N2 = axis of intermediate compressive stress, N3 = axis of least Compressive stress.

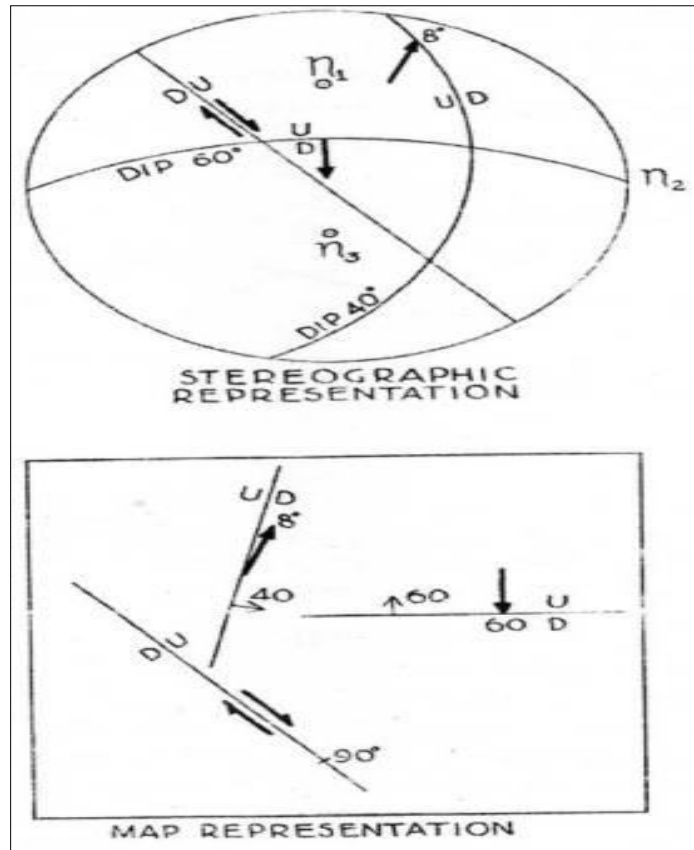


Figure.7 - Orientation of maximum shearing stress (*heavy arrows*) on three sample planes, in sample uniaxial compression, where axis of greatest compressive stress (N_1) plunges 30° to north, shown by stereographic projection and map representation.

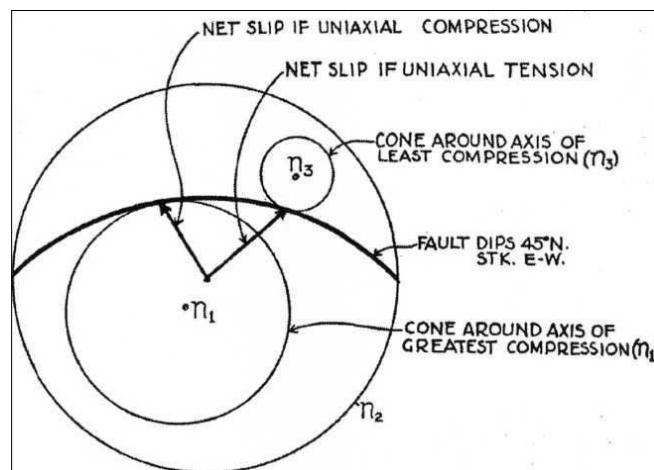


Figure.8 - Graphical determination of orientation of maximum shearing stress in simple tension and simple compression with any orientation of N_1 , N_2 , and N_3 . These two orientations serve as limits between which lie all possible orientations of maximum shearing stress on this plane with this stress system orientation, regardless of values of N_1 , N_2 , and N_3 .

Limitation

Although it is believed that the geometry of shearing stress described in this paper supplies an extremely useful basis for the interpretation of the Pachmarhi fault systems and the solution of some fault problems, it should be re-emphasized that the concept is limited

form here presented can be applied directly to faults in relatively few and special cases. It is felt that the importance lies in establishing a basis for a better three-dimensional concept of the elementary problem. The application of these principles to actual field problems will require the accounting of perhaps several more variables, and, although this poses very serious difficulties, it does not lessen the need for an adequate, three-dimensional concept of stress as a foundation upon which the other variables can be stacked.

References

- Anderson, E. M. (1948) On lineation and petro graphic structure and the shearing by which they have been produced : London Geol. Soc. Quart. Jour., vol. 104. pt, I, pp. 99-125.
- Bucher, W.H. (1921) the mechanical interpretation of joints: Jour, Geology vol. 29, pp. 1-28.
- Bucher, W.H. (1944) The stereographic projection, a handy tool for the practical geologist: *ibid.*, vol. 52, pp. 191-212.
- Fisher, D.J. (1941) A new projection protractor: Jour. Geology, vol. 40, pp. 292-323,420-444.
- Ford, W.E. (1932) Dana's textbook of mineralogy, New York, John Wiley & Sons, Inc., 851 pp.
- Griggs. D.T. (1936) Deformation of rocks under high confining pressure: Jour, Geology, vol. 44, pp. 541-577.
- Nadai. A. (1931) Plasticity, New York, McGraw-Hill Book Co., Inc., 149 pp.
- Sander, B. (1948) Einführung in die Gefugekunde der geologischen Korper, Berlin, Springer-Verlag.
- Schmidt, W., and Lindlev, H.W. (1938) Scherung: Min. pet. Mitt., vol. 50, pp. 1-28.
- Palchik, V. (2006), Stress–Strain Model for Carbonate Rocks Based on Haldane’s Distribution Function, *Rock Mech Rock Engng*, 39(3), 215.
- Riggs, Eric M. (2005), A new class of microstructures which lead to transformation-induced faulting in Magnesium germanate, *J Geophys Res*, 110, B03202.
- Wachter, L.M., C.E. Renshaw, and E.M. Schulson (2009), Transition in brittle failure mode in ice under low confinement, *Acta Mater*, 57(2), 345.
- Wong, Teng-fong, Robina H.C. Wong, K.T. Chau, and C.A. Tang (2006), Microcrack statistics, Weibull distribution and micromechanical modeling of compressive failure in rock, *Mech Mater*, 38(7), 664.
-